J|A|C|S
ARTICLES
Published on Web 03/14/2003

Formation of a PNA_2-DNA_2 Hybrid Quadruplex

Bhaskar Datta, Christoph Schmitt, and Bruce A. Armitage*

Contribution from the Department of Chemistry, Carnegie Mellon University, 4400 Fifth Avenue, Pittsburgh, Pennsylvania 15213-3890

Received August 28, 2002; E-mail: army@cyrus.andrew.cmu.edu

Abstract: DNA guanine (G) quadruplexes are stabilized by an interesting variation of the hydrogen-bonding schemes encountered in nucleic acid duplexes and triplexes. In an attempt to use this mode of molecular recognition, we target a dimeric G-quadruplex formed by the *Oxytricha nova* telomeric sequence $d(G_4T_4G_4)$ with a peptide nucleic acid (PNA) probe having a homologous rather than complementary sequence. UV−vis and CD spectroscopy reveal that a stable hybrid possessing G-quartets is formed between the PNA and DNA. The four-stranded character of the hybrid and the relative orientation of the strands is determined by fluorescence resonance energy transfer (FRET) experiments. FRET results indicate that (i) the two PNA strands are parallel to each other, (ii) the two DNA strands are parallel to each other, and (iii) the 5′-termini of the DNA strands align with the *N*-termini of the PNA strands. The resulting PNA_2-DNA_2 quadruplex shows a preference of Na^+ over Li^+ and displays thermodynamic behavior consistent with alternating PNA and DNA strands in the hybrid. The formation of this novel supramolecular structure demonstrates a new high-affinity DNA recognition mechanism and expands the scope of molecular recognition by PNA.

Introduction

Watson−Crick base-pairing of nucleic acids is one of the most elegant events of molecular recognition in nature and guarantees the storage, transfer and expression of genetic information in living systems. It forms the basis of therapeutic and diagnostic applications, especially in the form of antisense oligonucleotides.[1−4] So far, strategies for oligonucleotide modifications that have preserved the Watson−Crick base-pairing capability while changing the backbone (sugar and phosphate), have been more numerous and successful. Among such oligonucleotides, one of the most radical changes to the natural structure is in peptide nucleic acids (PNAs) where the entire sugar−phosphate backbone is replaced by a pseudopeptide.[5−7] PNA hybridizes with high affinity and sequence specificity to complementary DNA or RNA oligomers to form duplexes and triplexes by Watson−Crick and Hoogsteen base-pairing, respectively.[8−10] PNA also exhibits high chemical stability to protease and nuclease enzymes.[11] Although the hybridization of PNA probes to complementary DNA or RNA targets should be hindered by the presence of structure in the target sequences,[12] we recently reported the ability of short PNA probes to disrupt stable DNA hairpin[13] and quadruplex structures.[14]

Unlike RNA, the structural repertoire of DNA consists for the most part of the double helix with Watson−Crick base-pairing and to a lesser extent of other structures such as hairpins, triplexes, quadruplexes and cruciforms. There is growing interest in DNA quadruplexes as lead molecules in drug design[15−17] and as a structural motif potentially adopted by telomeres,[18,19] immunoglobin switch regions, centromere DNA and other biological systems.[20−22] DNA quadruplexes exist in various isomeric forms, built upon the motif of the guanine (G) quartet (Scheme 1).[23] This structure has four guanine bases held together

(1) Nielsen, P. E. *Curr. Opin. Struct. Biol.* **1999**, *9*, 353−357.
(2) Bennett, C. F. *Biochem. Pharmacol.* **1998**, *55*, 9−19.
(3) Mesmaeker, A. D.; Altmann, K.-H.; Waldner, A.; Wendeborn, S. *Curr. Biol.* **1995**, *5*, 343−355.
(4) *Encyclopaedia of Cancer*; Uhlmann, E., Peyman, A., Will, D. W., Eds.; Academic Press: San Diego, CA, 1997; Vol. 1.
(5) Nielsen, P. E.; Egholm, M.; Berg, R. H.; Buchardt, O. *Science* **1991**, *254*, 1498−1500.
(6) Uhlmann, E.; Peyman, A.; Breihpohl, G.; Will, D. W. *Angew. Chem., Int. Ed. Engl.* **1998**, *37*, 2796−2823.
(7) Nielsen, P. E.; Haaima, G. *Chem. Soc. Rev.* **1997**, *26*, 73−78.
(8) Giesen, U.; Kleider, W.; Berding, C.; Geiger, A.; Ørum, H.; Nielsen, P. E. *Nucleic Acids Res.* **1998**, *26*, 5004−5006.
(9) Egholm, M.; Buchardt, O.; Christensen, L.; Behrens, C.; Freier, S. M.; Driver, D. A.; Berg, R. H.; Kim, S. K.; Nordén, B.; Nielsen, P. E. *Nature* **1993**, *365*, 566−568.
(10) Ratilainen, T.; Holmen, A.; Tuite, E.; Haaima, G.; Christensen, L.; Nielsen, P. E.; Nordén, B. *Biochemistry* **1998**, *37*, 12 331−12 342.
(11) Demidov, V. V.; Potaman, V. N.; Frank- Kamanetskii, M. D.; Egholm, M. B.; O.; Sönnichsen, S. H.; Nielsen, P. E. *Biochem. Pharmacol.* **1994**, *48*, 1310−1313.
(12) Ørum, H.; Nielsen, P. E.; Jørgensen, M.; Larsson, C.; Stanley, C.; Koch, T. *BioTechniques* **1995**, *19*, 472−480.
(13) Kushon, S. A.; Jordan, J. P.; Seifert, J. L.; Nielsen, P. E.; Armitage, B. A. *J. Am. Chem. Soc.* **2001**, *123*, 10 805−10 813.
(14) Datta, B.; Armitage, B. A. *J. Am. Chem. Soc.* **2001**, *123*, 9612−9619.
(15) Bock, L. C.; Griffin, L. C.; Latham, J. A.; Vermaas, E. H.; Toole, J. J. *Nature* **1992**, *355*, 564−566.
(16) Paborsky, L. R.; McCurdy, S. N.; Griffin, L. C.; Toole, J. J.; Leung, L. L. *J. Biol. Chem.* **1993**, *268*, 20 808−20 811.
(17) Tasset, D. M.; Kubik, M. F.; Steiher, W. *J. Mol. Biol.* **1997**, *272*, 688−698.
(18) Williamson, J. R.; Raghuraman, M. K.; Cech, T. R. *Cell* **1989**, *59*, 871−880.
(19) Feigon, J.; Dieckmann, T.; Smith, F. W. *Chem. Biol.* **1996**, *3*, 611−617.
(20) Blackburn, E. H. *Cell* **1994**, *77*, 621−623.
(21) Greider, C. W.; Blackburn, E. H. *Sci. Am.* **1996**, *274*, 92−97.
(22) Marx, J. *Science* **1994**, *265*, 1656−1658.
(23) Guschlbauer, W.; Chantot, J. F.; Thiele, D. *J. Biomol. Struct. Dynam.* **1990**, *8*, 491−511.

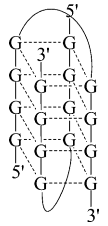

Figure 1. Quadruplex secondary structure of **G_4-DNA**. Solid and dashed lines indicate covalent and hydrogen bonding connections, respectively.

Scheme 1. G-quartet with Coordinated Na^+ Ion

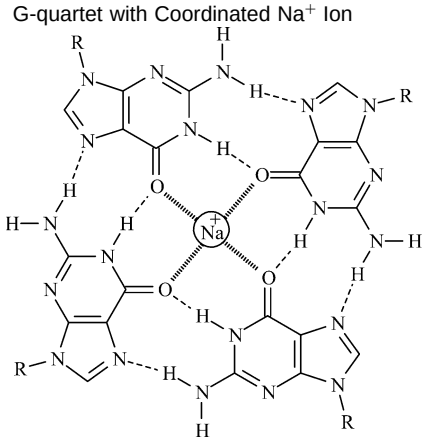

by means of Hoogsteen and Watson−Crick hydrogen-bonding.[24] The guanines may belong to one, two or four separate DNA strands producing quadruplexes with a variety of topologies. For example, the telomeric repeat region of the protozoan *Oxytricha nova* has the sequence d(T_4G_4) and associates to form a stable parallel four-stranded complex with four G-quartets.[25,26] In contrast, a longer section of the same telomere repeat sequence d($G_4T_4G_4$) forms a dimeric hairpin quadruplex structure with four G quartets (Figure 1).[27,28] The structure and stability of these G-quadruplexes is dependent on cations such as sodium and potassium.[24,25,29,30] Although the biological significance of such polymorphism is not understood, factors such as the length of G-clusters and intervening loops are critical to the formation of specific quadruplex conformations.[31,32]

Elements of G-quartet formation are also evident in RNA. For example, physiologically relevant RNA G-quartets are found in the filamentous bacteriophage fd.[33] Recently, the fragile X mental retardation protein (FMRP) has been shown to bind RNAs that form intramolecular G-quartets.[34] This process is believed to underlie the fragile X syndrome, the most common form of inherited human mental retardation. Thus, RNA G-quartets are most likely to be functionally important in living cells.

The novel supramolecular architecture of G-quartets has led to the development of interesting and functional noncovalent assemblies such as G-wires,[35] ion-channels[36] and self-assembled ionophores.[37] Though these applications often involve synthetically modified guanine nucleobases, nucleic acid analogues with different backbones have rarely been used for the same purpose. In particular, whether the guanine tetrad binding scheme could be used as a strategy for hybridization of probes to DNA has not been addressed. Though analogues such as PNA have been developed to mimic Watson−Crick and Hoogsteen base-pairing, they are expected to be in proper register for participating in G-tetrad formation as well. In an attempt to use this mode of molecular recognition we now report that homologous G-rich PNA and DNA oligomers hybridize to form a PNA_2−DNA_2 quadruplex. The hybrid quadruplex exhibits high thermodynamic stability and expands the range of molecular recognition motifs for PNA beyond duplex and triplex formation.

Experimental Section

Materials. Unmodified DNA oligonucleotides (purified by gel filtration chromatography) and fluorescein/Cy3 labeled oligonucleotides (purified by HPLC) were purchased from Integrated DNA Technologies, Inc. (http://www.idtdna.com). Concentrations were determined spectrophotometrically using the absorbance at 260 nm and literature values for extinction coefficients.[38] Absorbance measurements were made at 80 °C on a Cary 3 Bio spectrophotometer. The nucleobases are assumed to be completely unstacked at 80 °C, and the absorptivity is then assumed to be the sum of the absorptivities of the DNA monomers. PNA oligomers were synthesized using standard solid-phase synthesis protocols.[39,40] Boc/Z- protected PNA monomers were purchased from Perseptive Biosystems (Framingham, MA). Fluorescein-5-carboxylic acid was purchased from Molecular Probes, Inc. (Eugene, OR) and used without further purification. Cy3-carboxylic acid was a gift from Dr. Brigitte Schmidt (Carnegie Mellon University) and was coupled to the *N*-terminus of the PNA using HBTU. Boc protected Lys-MBHA resin was used, and the synthesis was performed on a 100 mg scale. All PNA probes (Chart 1) were purified using reversed-phase HPLC and characterized by MALDI-TOF spectrometry (**G_4-PNA**: *m*/*z* calculated 3542.2, observed 3542.2; ***N*-Fl** *m*/*z* calculated 3904.2, observed 3906.8; ***N*-Cy3** *m*/*z* calculated 4139.2, observed 4138.7). Stock solutions of the PNA were prepared in 10 mM sodium phosphate buffer (pH 7.0). Extinction coefficients for PNA monomers were obtained from Perseptive Biosystems ($C = 6600\ M^{-1}cm^{-1}$; $T = 8600\ M^{-1}cm^{-1}$; $A = 13\,700\ M^{-1}cm^{-1}$; $G = 11\,700\ M^{-1}cm^{-1}$).

Equipment. UV−vis measurements were performed on a Varian Cary 3 Bio spectrophotometer equipped with a thermoelectrically controlled multicell holder. Circular dichroism (CD) spectra were recorded on a Jasco J-715 spectropolarimeter with a thermoelectrically controlled single cell holder. Fluorescence experiments were performed on a PTI spectrofluorimeter with temperature controlled cell holder.

Sample Preparation. G_4-DNA was suspended in a buffer containing 10 mM sodium phosphate (pH 7.0), 100 mM NaCl and 0.1 mM EDTA, incubated at 90 °C for 10 min and slowly cooled to 25 °C to produce the dimeric, hairpin quadruplex structure. PNA hybridization was

(24) Williamson, J. R.; Raghuraman, M. K.; Cech, T. R. *Annu. Rev. Biophys. Biomol. Struct.* **1994**, *23*, 703−730.
(25) Sen, D.; Gilbert, W. *Nature* **1988**, *334*, 364−366.
(26) Lu, M.; Guo, Q.; Kallenbach, N. R. *Biochemistry* **1992**, *31*, 2455−2459.
(27) Smith, F. W.; Feigon, J. *Nature* **1992**, *356*, 164−168.
(28) Schultze, P. E.; Hud, N. V.; Smith, F. W.; Feigon, J. *Nucleic Acids Res.* **1999**, *27*, 3018−3028.
(29) Hardin, C. C.; Henderson, E.; Watson, T.; Prosser, J. K. *Biochemistry* **1991**, *30*, 4460−4472.
(30) Miura, T.; Benevides, J. M.; Thomas, G. J., Jr. *J. Mol. Biol.* **1995**, *248*, 233−238.
(31) Guo, Q.; Lu, M.; Kallenbach, N. R. *Biochemistry* **1993**, *32*, 3596−3603.
(32) Smirnov, I.; Shafer, R. H. *Biochemistry* **2000**, *39*, 1462−1468.
(33) Oliver, A. W.; Bogdarina, I.; Schroeder, E.; Taylor, I. A.; Kneale, G. G. *J. Mol. Biol.* **2000**, *301*, 575−584.
(34) Darnell, J. C.; Jensen, K. B.; Jin, P.; Brown, V.; Warren, S. T.; Darnell, R. B. *Cell* **2001**, *107*, 489−499.
(35) Marsh, T. C.; Vesenka, J.; Henderson, E. *Biochemistry* **1994**, *33*, 10 718−10 724.
(36) Forman, S. L.; Fettinger, J. C.; Pieraccini, S.; Gottarelli, G.; Davis, J. T. *J. Am. Chem. Soc.* **2000**, *122*, 4060−4067.
(37) West, R. T.; Garza, L. A.; Winchester, W. R.; Walmsley, J. A. *Nucleic Acids Res.* **1994**, *22*, 5128−5134.
(38) Dawson, R. M. C.; Elliott, D. C.; Elliott, W. H.; Jones, K. M. *Data for Biochemical Research*; Oxford University Press: New York, 1986.
(39) Christensen, L.; Fitzpatrick, R.; Gildea, B.; Petersen, K. H.; Hansen, H. F.; Koch, T.; Egholm, M.; Buchardt, O.; Nielsen, P. E.; Coull, J.; Berg, R. H. *J. Peptide Sci.* **1995**, *3*, 175−183.
(40) Koch, T.; Hansen, H. F.; Andersen, P.; Larsen, T.; Batz, H. G.; Otteson, K.; Orum, H. *J. Peptide Res.* **1997**, *49*, 80−88.

Chart 1 PNA and DNA Sequences. Fluorophore Structures and Linkages Are Shown Below

Name	Sequence
G_4-DNA	5'-GGGGTTTTGGGG-3'
G_4-PNA	H-GGGGTTTTGGGG-Lys-NH_2
5'-Fl (DNA)	5'-Fluorescein-GGGGTTTTGGGG-3'
3'-Fl (DNA)	5'-GGGGTTTTGGGG-Fluorescein-3'
5'-Cy3 (DNA)	5'-Cy3-GGGGTTTTGGGG-3'
N-Fl (PNA)	Fluorescein-GGGGTTTTGGGG-Lys-NH_2
N-Cy3 (PNA)	Cy3-GGGGTTTTGGGG-Lys-NH_2

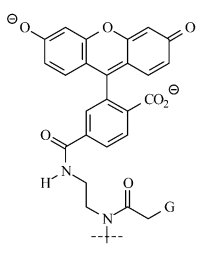

***N*-Fl-PNA**

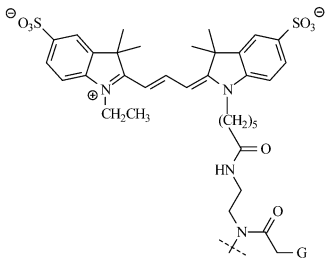

***N*-Cy3-PNA**

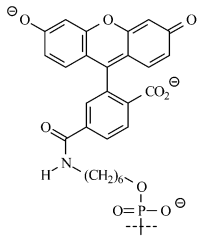

5'-Fl-DNA

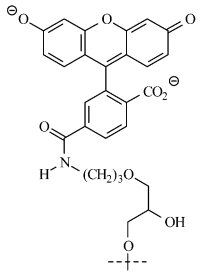

3'-Fl-DNA

accomplished by adding PNA to the quadruplex (5.0 μM each) in a buffer containing 10 mM sodium phosphate (pH 7.0), 100 mM NaCl and 0.1 mM EDTA. Experiments were then performed immediately after mixing at room temperature or after subsequently heating to 90 °C for five min, then cooling to 25 °C (annealing).

Circular Dichroism Analysis. Proper folding of the DNA quadruplex and hybridization by PNA were monitored using CD spectropolarimetry. All spectra represent an average of eight scans collected at a rate of 100 nm/min. All spectra were baseline subtracted and smoothed via a five point adjacent averaging algorithm.

Continuous Variations Experiment. Samples containing variable amounts of PNA and DNA (total concentration, 10.0 μM) were annealed in a buffer containing 10 mM sodium phosphate (pH 7.0), 100 mM NaCl and 0.1 mM EDTA. CD spectra were recorded at 25 °C after equilibration for 15 min and the signal at 260 nm was plotted versus the mole fraction of PNA.

Fluorescence Studies. Samples containing 1.0 μM each of labeled and unlabeled strands, as specified below, were annealed in a buffer containing 10 mM sodium phosphate (pH 7.0), 100 mM NaCl and 0.1 mM EDTA. Fluorescence spectra were measured with excitation at 450 nm, where excitation of Cy3 is minimal. All of the spectra were recorded at 25 °C with a 4 nm band-pass on both the excitation and emission monochromators. Ten scans were recorded and averaged. The emission intensity at the donor maximum (515 nm for Fl-DNA and 521 nm for Fl-PNA) was measured in donor-only (I_D) and donor−acceptor (I_{DA}) hybrids. The cyanine acceptor has negligible emission at these wavelengths. To measure FRET efficiency between DNA strands, samples containing one equivalent each of 5′-Fl and 5′-Cy3 DNA along with two equivalents of unlabeled PNA were annealed. In this case, the maximum FRET efficiency is 50% because only half of the hybrids containing a 5′-Fl DNA strand will also have a 5′-Cy3 DNA strand. The same reasoning applies to the other experiments performed where only one type of strand is labeled (3′-Fl/5′-Cy3 DNA and *N*-Fl/*N*-Cy3 PNA). For experiments in which both the PNA and DNA strands are labeled, samples contained one equivalent each of the labeled strands and one equivalent each of the unlabeled strands. Therefore, in these experiments, there is a 75% chance that a hybrid having a fluorescein label will also contain at least one Cy3 label, meaning that maximum FRET efficiency in these cases is 75%. The data shown in Table 1 and described in the text are corrected for these statistical factors.

Table 1. Fluorescence Resonance Energy Transfer Efficiencies for Labeled PNA/DNA Hybrids

labeled strands	donor	acceptor	FRET efficiency[a]
DNA/DNA	5′-Fl	5′-Cy3	0.80 ± 0.01
DNA/DNA	3′-Fl	5′-Cy3	0.34 ± 0.01
PNA/PNA	*N*-Fl	*N*-Cy3	1.00 ± 0.01
PNA/DNA	*N*-Fl	5′-Cy3	0.91 ± 0.02
PNA/DNA	5′-Fl	*N*-Cy3	0.68 ± 0.02
PNA/DNA	3′-Fl	*N*-Cy3	0.44 ± 0.01

[a] Values are averages ± standard deviations of three independent trials and are corrected for statistical formation of unlabeled duplexes as described in the Experimental section.

The efficiency of energy transfer (E) was calculated by the quenching of donor emission in the presence of the acceptor as

$$E = 1 - I_{DA}/I_D$$

Thermal Analysis. Samples were prepared in a buffer containing 10 mM sodium phosphate (pH 7.0), 0.1 mM EDTA and variable amounts of NaCl or LiCl. Unless otherwise indicated, samples were heated to 90 °C and equilibrated for 5 min. UV−vis absorbance at 295 nm and CD intensity at 295 nm were recorded every 0.5 °C as samples were cooled and then heated at 1.0 °C/min. (Experiments performed at 0.5 °C/min yielded similar results.) Experiments were done in triplicate; the values in data tables reflect the averages of those measurements. Heating curves were corrected for sloping baselines prior to determining the melting temperature (T_m) as the midpoint of the transition. Thermodynamic parameters were determined from curve-fitting data from heating ramps.[43] In one case, concentration dependent method of analysis yielded thermodynamic parameters that were within 10% of those obtained by the shape-fitting method of analysis.

Results

Target Selection. The 12-base DNA sequence 5′-G_4-T_4-G_4-3′ (**G_4-DNA**, Chart 1) contains a G-rich sequence from the *Oxytricha nova* telomere. Under various conditions, this sequence can assemble into a bimolecular hairpin quadruplex with diagonal loop conformations (Figure 1).[25,26] Multiple stacked G-tetrads, each of which involves the formation of eight hydrogen bonds, stabilize the structure. This secondary structure is stabilized by the presence of moderate sodium ion concentrations and has been verified in solution by multidimensional NMR spectroscopy,[27,28] making it an attractive starting point for our investigations of how G-rich PNA would recognize such DNA sequences.

Characterization of G_4-DNA. Annealing of G_4-DNA was performed as described in the Experimental section. Formation

(41) Williamson, J. R. *Curr. Opin. Struct. Biol.* **1993**, *3*, 357−362.
(42) Balagurumoorthy, P.; Brahmachari, S. K.; Mohanty, D.; Bansal, M.; Sasisekharan, V. *Nucleic Acids Res.* **1992**, *20*, 4061−4067.
(43) Marky, L. A.; Breslauer, K. J. *Biopolymers* **1987**, *26*, 1601−1620.

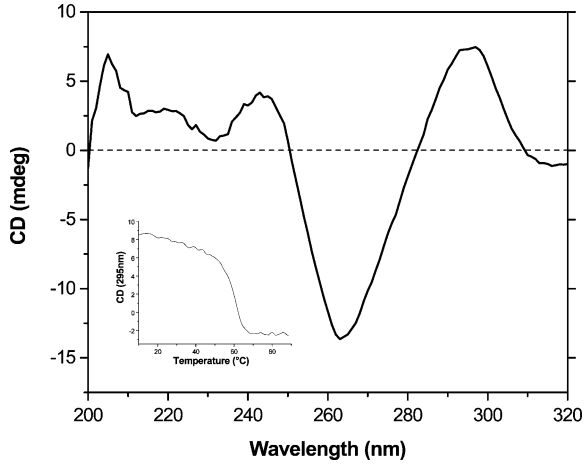

Figure 2. CD spectrum of **G_4-DNA** (5.0 μM) at 25 °C. Eight scans were collected at a rate of 100 nm/min and averaged. Inset: CD melting profile of **G_4-DNA** monitored at $\lambda = 295$ nm.

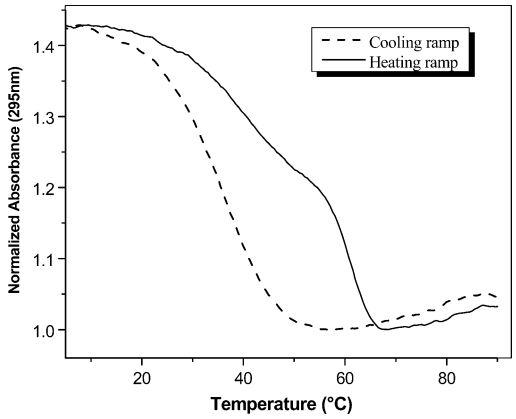

Figure 3. UV−vis melting profile recorded at $\lambda = 295$ nm of **G_4-DNA** (5.0 μM). Cooling ramp (dashed line) and heating ramp (solid line) were scanned at a rate of 1 °C/min.

of the desired quadruplex was confirmed by a circular dichroism (CD) spectrum, which matched the literature spectrum for this sequence. In particular, the CD spectrum showed a maximum at 295 nm and minimum at 265 nm (Figure 2); signature bands for antiparallel quadruplexes.[41,42] The CD maximum at 295 nm was used to monitor the dissociation of the quadruplex upon heating. The quadruplex displayed a cooperative dissociation with a "melting temperature" (T_m) of 61.5 °C (inset, Figure 2).

Previously, Mergny et al. reported the use of 295 nm as a signature wavelength for precisely monitoring intra- or intermolecular G-quartet formation and dissociation by UV spectroscopy.[44] We performed melting experiments on **G_4-DNA** monitored at 295 nm and observed two distinct transitions in the dissociation (heating) curve, as well as a substantial hysteresis (Figure 3). We do not have an explanation for the upward sloping baseline observed at high temperature, although Mergny and co-workers also saw this phenomenon for a different G-quadruplex monitored at 295 nm.[44] We note that this effect is not observed in the CD melting curve recorded at the same wavelength (Figure 2). There was little change in the hysteresis or nature of transitions when the thermal analysis experiment was carried out at 275 nm (data not shown). The T_m obtained from the higher temperature transition on the

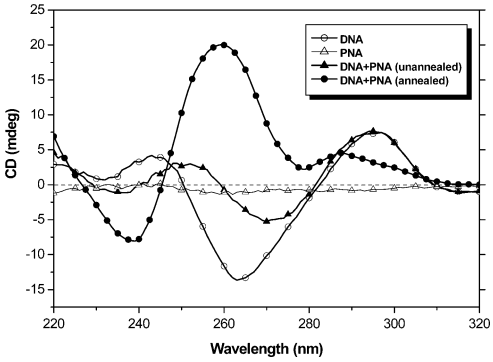

Figure 4. CD spectra of 5.0 μM **G_4-DNA** (open circles), 5.0 μM **G_4-PNA** (open triangles), and a 1:1 mixture of **G_4-DNA** and **G_4-PNA** (5.0 μM each) before (filled triangles) and after (filled circles) annealing. All spectra were measured at 25 °C and represent the average of eight scans collected at 100 nm/min.

heating curve was identical to that calculated from CD. The complex UV-melting behavior suggests different folding/unfolding pathways for the oligonucleotides. We speculate the hysteresis to be arising from a difference in kinetics of association versus dissociation, as is often observed in the assembly of multistranded nucleic acid structures.[45,46] Although hysteresis is generally absent from simple Watson−Crick duplex systems, the bimolecular quadruplex structure formed by **G_4-DNA** requires that the two strands each fold into hairpins and assemble the G-quartets in the diagonal conformation shown in Figure 1, so it is perhaps not surprising that the association kinetics might be considerably slower.

Hybridization of G_4-PNA with G_4-DNA. To study the hybridization of PNA with **G_4-DNA** using G-tetrads, **G_4-PNA** bearing the same sequence as **G_4-DNA** (Chart 1) was synthesized using standard solid-phase peptide synthesis protocols.[39,40] Purine-rich PNAs are believed to be problematic in terms of solubility and aggregation properties. For example, typing the **G_4-PNA** sequence into the PNA Probe Designer software on the Applied Biosystems website (http://www.appliedbiosystems.com/support/pnadesigner.cfm) leads to the recommendation that the sequence be redesigned due to problems normally encountered with synthesizing PNAs having >60% purine content. We had no difficulties in the synthesis, purification, or handling of this sequence, however.

To characterize the interaction of **G_4-PNA** with **G_4-DNA**, several experiments were performed. First, CD spectra were recorded for **G_4-DNA** alone, **G_4-PNA** alone and a 1:1 mixture of the two (Figure 4). Although the spectrum of the mixture is not simply the sum of the individual components, it retains essential signatures of antiparallel quadruplexes, most notably the positive band at 295 nm.

Although no striking changes were observed in the CD spectrum of the unannealed mixture of **G_4-DNA** and **G_4-PNA**, annealing the sample produced a dramatically different CD (Figure 4). The spectrum with a maximum at 260 nm and a minimum at 240 nm is characteristic of parallel DNA quadruplexes.[47] A continuous variations experiment using the CD maximum at 260 nm, demonstrates that the interaction between

(44) Mergny, J.-L.; Phan, A.-T.; Lacroix, L. *FEBS Lett.* **1998**, *435*, 74−78.
(45) Griffith, M. C.; Risen, L. M.; Grieg, M. J.; Lesnik, E. A.; Sprankle, K. G.; Griffey, R. H.; Kiely, J. S.; Freier, S. M. *J. Am. Chem. Soc.* **1995**, *117*, 831−832.
(46) Hoff, A. J.; Roos, A. L. M. *Biopolymers* **1972**, *11*, 1289−1294.
(47) Giraldo, R.; Suzuki, M.; Chapman, L.; Rhodes, D. *Proc. Natl. Acad. Sci. U.S.A.* **1994**, *91*, 7658−7662.

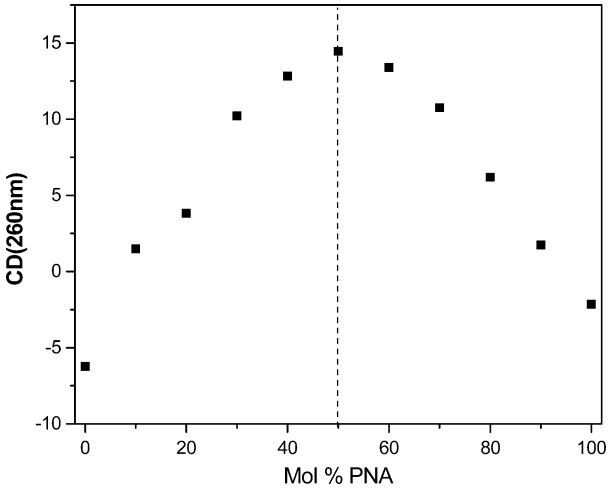

Figure 5. Continuous variations experiment of **G_4-DNA/G_4-PNA** hybridization. The total strand concentration was held constant at 10.0 μM and the CD intensity at $\lambda = 260$ nm was recorded from spectra recorded as described in Figure 4.

G_4-PNA and **G_4-DNA** yields a complex with 1:1 stoichiometry (Figure 5). This binding stoichiometry is empirical since higher order structures are possible for G-rich oligonucleotides. Notably, four-stranded DNA quadruplexes have been reported extensively;[47−49] an analogous structure in the present case would then consist of two PNA and two DNA strands.

Hybrid Composition and Strand Orientation. We next used fluorescence resonance energy transfer (FRET) experiments to determine whether the hybrids contained one or more DNA and PNA strands as well as their relative orientations within the complex. **G_4-PNA** labeled at the *N*-terminus with either fluorescein (Fl) or Cy3 were synthesized (Chart 1) using modified solid-phase synthesis protocols. DNA oligomers bearing 5′- or 3′-Fl or 5′-Cy3 labels were purchased. In these experiments, the Fl and Cy3 fluorophores function as energy donor and acceptor groups, respectively. The fluorophores did not perturb either the CD spectrum or the UV melting curve for the hybrid (data not shown).

In the first experiment, two hybrids were prepared. Both samples contained one equivalent of 5′-Fl-DNA and two equivalents of unlabeled **G_4-PNA**. One sample also contained one equivalent of unlabeled DNA, while the other contained one equivalent of 5′-Cy3-DNA. As shown in Figure 6A, 40% energy transfer, was observed in the presence of Cy3-labeled DNA. Note that theoretically, the maximum efficiency is 50%, given that a 1:1 ratio of Fl- and Cy3-labeled DNA was used, meaning that the actual FRET efficiency is 80% after correcting for statistical factors (Table 1). This result demonstrates that at least two DNA strands are present in the hybrid. A similar experiment in which the PNA strands were labeled with Fl and Cy3 at the *N*-terminus, whereas the DNA strand remained unlabeled resulted in 50% energy transfer (Figure 6B), i.e., the theoretical maximum, verifying that at least two PNA strands are also present in the hybrid. Based on these results, the simplest stoichiometry for the hybrid is PNA_2-DNA_2.

Three sets of experiments were performed to ascertain the relative orientation of DNA and PNA strands in the hybrid (Table 1). First, a hybrid was prepared containing 3′-Fl and 5′-Cy3 DNA along with unlabeled PNA. The resulting complex exhibited only 17% energy transfer (34% of the theoretical maximum), significantly lower than what was observed when both DNA strands were labeled at the 5′-end (Table 1). This indicates that the two DNA strands are oriented parallel to one another in the hybrid.

Next, to understand the orientation of DNA relative to PNA, the *N*-terminal Cy3-PNA was mixed with either 5′-Fl or 3′-Fl-DNA. In this experiment, one equivalent of each labeled strand were mixed with one equivalent of each unlabeled strand. Thus, each quadruplex will contain zero, one or two Cy3-labeled PNA strands, in a 1:2:1 statistical ratio. This means that the maximum FRET efficiency for these experiments is 75%. The observed energy transfer efficiency was 51% (68% of maximum) when the fluorescein was on the DNA 5′-terminus, but decreased to 33% (44% of maximum) for the 3′-Fl DNA, indicating that the PNA *N*-terminus aligns with the DNA 5′-terminus. This stands in contrast to the well-known preference of PNA to align its *N*-terminus with the DNA 3′-terminus when hybridizing by Watson−Crick base pairing. When the labels are switched so that the fluorescein is on the PNA strand and the Cy3 is on the DNA strand, the FRET efficiency remains high (68%, 91% of maximum). The higher FRET efficiency in this case could arise from the shorter linker connecting fluorescein to the PNA strand relative to that used for the DNA strand.

Finally, regarding the relative orientation of the two **G_4-PNA** strands, we note that a FRET efficiency of 50% was observed between *N*-Fl/*N*-Cy3 (Figure 6B and Table 1). This is the maximum theoretical efficiency and indicates a parallel alignment of the PNA strands, resulting in the donor and acceptor labels being on the same end of the hybrid.

Thermodynamic Analysis of the PNA_2-DNA_2 Hybrid. UV-melting curves were used to characterize the thermodynamic stability of the **(G_4-PNA)**$_2$−**(G_4-DNA)**$_2$ hybrid. These experiments were performed at 295 nm; this wavelength has been used for exclusively monitoring DNA G-quartet association/dissociation processes.[44] Sequences unable to form G-quartets have been found to display negligible hyperchromicity at this wavelength. We observe smooth transitions characterized by large hyperchromicity (30%) and minimal hysteresis (Figure 7), suggesting that the assembly is in fact held together by G-quartets. Curve fitting by the method of Marky and Breslauer[43] yielded the free energy, enthalpy, and entropy of formation as shown in Table 2. We also analyzed the hybrid denaturation by using the concentration dependence of the melting temperature, and the thermodynamic parameters obtained by this method agreed with those by the curve-fitting procedure to within 10%, confirming the transition to be a two-state process (Table 2 and Figure S1).[43] On the basis of the FRET experiments described above, a molecularity of 4 was used for calculating thermodynamic parameters for the hybrid. In addition, **G_4-DNA** and **G_4-PNA** were treated as non self-complementary and the corresponding expression for the equilibrium used.[43] This selection is justified in the Discussion section. These parameters revealed a very high free energy of formation for the hybrid ($\Delta G_{298} = -37.3$ kcal/mol), comparable to results from a study by Kallenbach and co-workers on a parallel, 4-stranded DNA quadruplex formed by the sequence 5′-(G_4T)-3′, $\Delta G = -35.5$ kcal/mol.[31]

(48) Parkinson, G. N.; Lee, M. P. H.; Neidle, S. *Nature* **2002**, *417*, 876−880.
(49) Laughlan, G.; Murchie, A. I. H.; Norman, D. G.; Moore, M. H.; Moody, P. C. E.; Lilley, D. M. J.; Luisi, B. *Science* **1994**, *265*, 520−524.

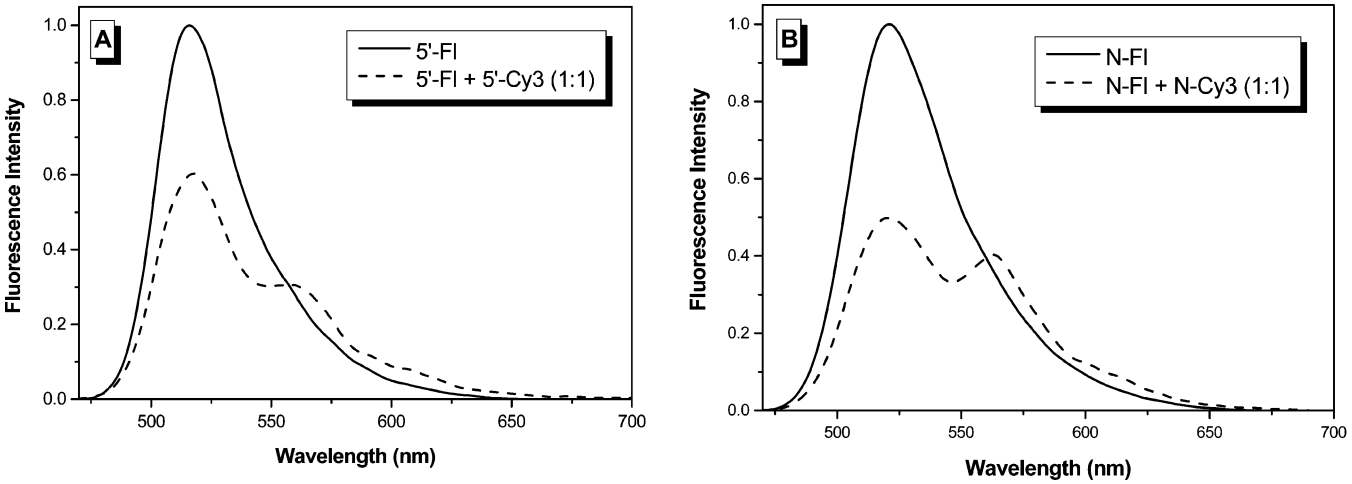

Figure 6. Fluorescence spectra of labeled **G_4-PNA** + **G_4-DNA** hybrids. (A) 1.0 μM 5′-Fl + 1.0 μM **G_4-DNA** + 2.0 μM **G_4-PNA** (solid line); 1.0 μM 5′-Fl + 1.0 μM 5′-Cy3 + 2.0 μM **G_4-PNA** (dashed line). (B) 1.0 μM N−Fl + 1.0 μM **G_4-PNA** + 2.0 μM **G_4-DNA** (solid line); 1.0 μM N−Fl + 1.0 μM N−Cy3 + 2.0 μM **G_4-DNA** (dashed line).

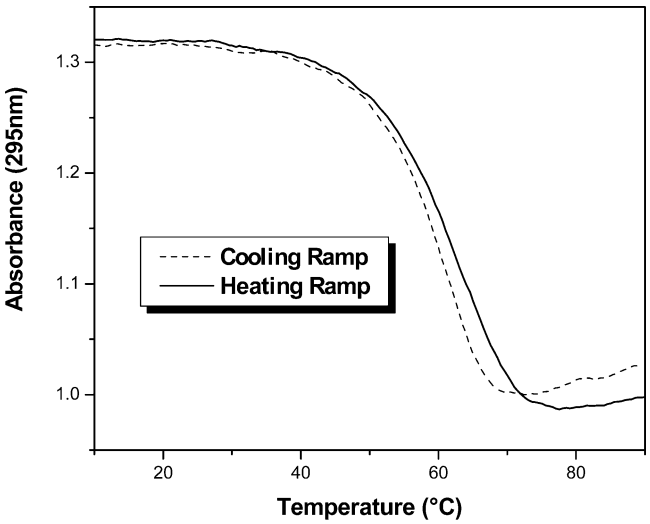

Figure 7. UV−vis melting profile of the PNA_2−DNA_2 hybrid quadruplex (5.0 μM of each strand). Cooling ramp (dashed line) and heating ramp (solid line) were recorded at λ = 295 nm at the rate of 1 °C/min.

Table 2. Effect of Ionic Strength on Thermodynamics of PNA_2-DNA_2 Quadruplex Formation[a]

[NaCl] (mM)	T_m (°C)	ΔG_{298}	ΔH (kcal/mol)	$T\Delta S_{298}$ (kcal/mol)
10	64.2 ± 0.2	−36.1 ± 0.5	−102.8 ± 2.4	−66.7 ± 1.9
100	65.4 ± 0.3	−37.3 ± 0.5	−110.6 ± 2.8	−73.3 ± 2.3
250	66.2 ± 0.2	−37.7 ± 0.5	−112.3 ± 2.6	−74.6 ± 2.1

[a] Values are averages ± standard deviations of three independent trials.

Ion Dependence of Hybrid Stability. DNA quadruplexes are known to display marked dependence on the nature of added metal ions and the ionic strength of the aqueous medium.[24] As would be expected from polyelectrolyte theory, these structures exhibit higher stability with increasing ionic strength of the solution,[50−52] but this behavior is also observed for simple Watson−Crick duplexes. The bimolecular quadruplex formed by **G_4-DNA** in the absence of the homologous PNA shows a significant stabilization in higher ionic strength buffer (ΔT_m = 5 °C in the presence of 250 mM NaCl versus 10 mM NaCl; data not shown) but the corresponding (**G_4-PNA**)$_2$−(**G_4-DNA**)$_2$ quadruplex is affected significantly less (ΔT_m = 2 °C; Table 2). This result indicates that the anionic phosphate backbones in the hybrid are further away from one another than in the bimolecular quadruplex, reducing the electrostatic repulsions and, therefore, the ionic strength dependence.

Table 3. Effect of Li^+ on Thermodynamics of PNA/DNA Quadruplex Formation

ion	T_m (°C)	ΔG_{298}	ΔH (kcal/mol)	$T\Delta S_{298}$ (kcal/mol)
Na^+	66.2 ± 0.2	−37.7 ± 0.5	−112.3 ± 26.6	−74.6 ± 2.1
Li^+	44.6 ± 0.1	−29.8 ± 0.1	−93.1 ± 1.2	−63.3 ± 1.1

Samples contained 10 mM NaCl plus 240 mM additional NaCl or LiCl.

A unique feature of the G-tetrad is the central pocket lined by electronegative carbonyl oxygens, which is the site of interaction with a cation.[24] This interaction is cation-specific due to the size of cavity between tetrads, leading to a preference for sodium or potassium over lithium. In the PNA−DNA quadruplex, inclusion of 240 mM LiCl along with 10 mM NaCl destabilizes the hybrid (ΔT_m = −21 °C, Table 3 and Figure S2). The substantial decrease in melting temperature of the hybrid indicates a preference of Na^+ as compared to Li^+ that may be attributed to cavity size between G-tetrads of the hybrid. Thus, whereas the **G_4-DNA** strands may not be in direct contact in the hybrid thereby reducing the effect of ionic strength on hybrid stability, the presence of G-tetrads formed between the G_4-PNA and G_4-DNA retains the dependence on the size of the monovalent cation.

Discussion

Structural Model for a PNA_2-DNA_2 Hybrid Quadruplex. The hydrogen-bonding pattern used to form guanine tetrads is a combination of Watson−Crick and Hoogsteen pairing. Previous work has shown that PNA is capable of binding to DNA targets using both of these recognition modes in the formation of PNA−DNA duplexes[53] and PNA_2−DNA triplexes.[54] Thus, it is reasonable to expect that PNA should be able to participate

(50) Manning, G. S. *J. Chem. Phys.* **1969**, *51*, 924−933.
(51) Manning, G. S. *Biopolymers* **1972**, *11*, 937−949.
(52) Record, M. T., Jr. *Biopolymers* **1975**, *14*, 2137−2158.
(53) Eriksson, M.; Nielsen, P. E. *Nat. Struct. Biol.* **1996**, *3*, 410−413.
(54) Betts, L.; Josey, J. A.; Veal, J. M.; Jordan, S. R. *Science* **1995**, *270*, 1838−1841.

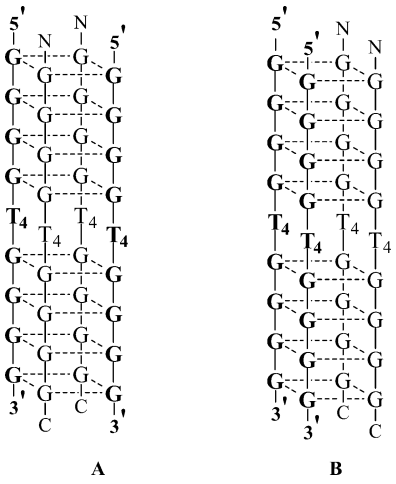

Figure 8. Possible structures of a PNA$_2$−DNA$_2$ hybrid quadruplex. DNA (bold) or PNA strands are (A) diagonally opposite or (B) adjacent to each other.

in G-quadruplex formation with DNA. Nevertheless, the present study is the first example of a PNA probe binding a DNA target by using the G-tetrad mode of molecular recognition and differs from all previous studies in that the PNA probe is homologous rather than complementary to the DNA target.

Formation of a PNA−DNA hybrid is revealed by a combination of CD, UV-thermal and fluorescence studies. The destabilization of the hybrid observed when Na^+ is replaced by Li^+ provides strong evidence in support of G-quartet formation. UV thermal denaturation of the hybrid monitored at 295 nm exhibits significant hyperchromicity, indicating that multiple G-quartets are stacked within the hybrid. The empirical 1:1 binding stoichiometry between DNA and PNA is consistent with formation of a hybrid quadruplex, whereas the CD spectrum of the hybrid is most similar to that of four-stranded parallel DNA quadruplexes. Hence, the most likely structure consists of 2 **G$_4$-PNA** and 2 **G$_4$-DNA** strands. This composition of the hybrid is consistent with FRET experiments described above (Table 1), which indicated that at least two DNA and two PNA strands are present, as well as by the close correspondence between the thermodynamic parameters obtained from independent curve fitting and concentration-dependence analyses. Moreover, the relative orientations of the **G$_4$-DNA** and **G$_4$-PNA** strands are revealed by the differences in energy transfer efficiencies for hybrids with 5′-Fl compared to 3′-Fl (Table 1). Although it is possible that the different efficiencies arise from different orientation factors for the donor/acceptor pairs, the long linkers used to attach the fluorescein donor to the 5′- or 3′-ends of **G$_4$-DNA** should provide sufficient flexibility that a random orientation can be assumed. Moreover, we see no effect of the fluorescein label on the T_m of the hybrid quadruplex, indicating that the fluorescein does not interact appreciably with the quadruplex. Therefore, we interpret the FRET results to indicate that the two DNA strands are parallel to each other, the two PNA strands are parallel to each other, and the 5′-termini of the DNA strands align with the *N*-termini of the PNA strands.

Two possible structures can be envisioned for a four-stranded PNA$_2$-DNA$_2$ hybrid (Figure 8). Of these, we consider the alternating structure (A) more likely for two reasons. First, the two anionic DNA strands are further apart than in structure (B), minimizing electrostatic repulsions. Second, FRET experiments in which the DNA and PNA are both labeled consistently give higher energy transfer efficiencies than the analogous experiments in which only the DNA or only the PNA strands are labeled. This indicates that the donor and acceptor are, on average, closer to one another when the PNA and DNA strands are both labeled.

Thermodynamic Analysis of PNA-DNA Quadruplex Formation. On the basis of the structure shown in Figure 8A, we calculated the thermodynamic parameters for assembly of the hybrid quadruplex using the method of Marky and Breslauer (Table 2).[43] In the calculations, the molecularity of the hybrid was taken to be four and the system was treated as nonself-complementary because, while all strands of the hybrid quadruplex have the same sequence, neither the two PNA nor the two DNA strands are bonded directly to each other if the alternating model shown in Figure 8 is correct.

An interesting observation from the melting studies concerns hysteresis in the thermal transitions. Specifically, the two-stranded hairpin dimer formed by **G$_4$-DNA** by itself exhibits a substantial hysteresis (Figure 3), whereas the four-stranded hybrid PNA$_2$-DNA$_2$ quadruplex exhibits almost no hysteresis (Figure 7). Structures having more than two strands such as triplexes will often show hysteresis while standard Watson−Crick duplexes typically do not. This is attributed to the slower kinetics of hybridization to form termolecular (or higher order) structures, leading to a lower transition temperature derived from cooling curves compared with heating curves. Although the hairpin dimer structure adopted by **G$_4$-DNA** is double-stranded, the kinetics of formation are likely retarded by the need for two hairpins to effectively invade one another, because all of the G−G hydrogen bonding is intermolecular. Nevertheless, the minimal hysteresis evident in formation of the four-stranded hybrid structure is surprising. It is possible that the hybridization kinetics are accelerated by the lack of negative charges along the backbone as well as the presence of terminal positive charges on the PNA strand.

The PNA$_2$−DNA$_2$ quadruplex exhibits very high thermodynamic stability: $\Delta G = -36.1$ kcal/mol at 10 mM NaCl. This is comparable to the stability of a four stranded DNA quadruplex formed by the sequence 5′-TGGGG-3′ and reported by Kallenbach and co-workers.[31] The stability of pure DNA quadruplexes depends strongly on the ionic strength due to electrostatic repulsion of the juxtaposed negatively charged strands in the quadruplex.[55] In the case of the hybrid quadruplex, the lack of direct association between the two DNA strands in the proposed structure is expected to attenuate the ionic strength dependence. In fact, an increase of NaCl concentration from 10 mM to 250 mM leads to only slightly enhanced stability ($\Delta\Delta G = -1.6$ kcal/mol). The small stabilization observed in this case could be due simply to enhanced screening of any residual electrostatic repulsions between the two DNA strands within the hybrid quadruplex.

Previous work demonstrated that **G$_4$-DNA** does not fold into a stable quadruplex structure in the presence of Li^+, presumably due to the small diameter of this cation relative to the cation binding pocket in G-quadruplex structures.[24] The hybrid PNA−DNA quadruplex displays a similar preference of Na^+ over Li^+ (Table 3). In particular, whereas 250 mM NaCl stabilizes the quadruplex relative to 10 mM NaCl ($\Delta\Delta G = -1.6$ kcal/mol;

(55) Miyoshi, D.; Nakao, A.; Toda, T.; Sugimoto, N. *FEBS Lett.* **2002**, *496*, 128−133.

$\Delta T_m = 2.0$ °C), the quadruplex is significantly destabilized by the addition of 240 mM LiCl ($\Delta\Delta G = 6.3$ kcal/mol; $\Delta T_m = -21.5$ °C). The stabilization by Na^+ and destabilization by Li^+ are enthalpic in origin, as would be expected from stronger counterion association of Na^+ compared to Li^+. A thorough study of ion association with the hybrid quadruplex will be the subject of a future report.

Implications. The initial excitement generated by PNA was due primarily to its ability to invade double helical DNA and bind its complementary target sequence.[5] Since then, PNA invasion of intramolecular hairpin[12,13,56] and quadruplex[14] targets has been reported. The hybridization reaction described here constitutes a new invasion pathway, in which a PNA disrupts a quadruplex tertiary structure to form a hybrid quadruplex with its homologous sequence. The high affinity with which G-rich PNA hybridizes to homologous DNA suggests numerous biological applications, particularly given the high chemical and enzymatic stability of the PNA structure. C-rich PNA complementary to human telomeric DNA has been used to image telomeres by fluorescence microscopy.[57,58] In principle, homologous G-rich PNA could be used for similar experiments, although formation of parallel four-stranded structures as described here may be precluded by the lack of accessibility to a second nearby telomere or by a telomere-binding protein. In addition to telomeric DNA, there is growing interest in the involvement of G-quadruplexes in diverse gene expression regulatory pathways. For example, several recent studies point toward the binding of the fragile X mental retardation protein (FMRP) to intramolecular quadruplex structures formed in mRNAs as critical for normal development.[59−61] Mutations that block expression of FMRP remove repression of these mRNAs and cause abnormal development. Separately, Hurley and co-workers provide compelling evidence for a G-quadruplex formed within chromosomal DNA upstream of the *c-Myc* gene linked to several cancers.[62] This report is particularly intriguing as it necessarily requires that the two DNA strands be locally separated in order for the intramolecular G-quadruplex to form. In this case, a homologous PNA could either hybridize with the G-rich strand to form a quadruplex or to the C-rich strand to form a duplex.

In order for G-rich PNA to be useful in biological systems, more must be learned about the range of structures and stoichiometries for complexes that can be formed with homologous DNA and RNA sequences. For example, in the absence of folding, an isolated DNA strand would require three PNA strands to form a stable quadruplex. The data shown in Figure 5 show no evidence for a 3:1 complex, but this does not rule out the possibility that other sequences could do so. Alternatively, PNA sequences that can form 1:1 complexes analogous to the purely DNA hairpin dimer targeted in this study could be of great utility. We are currently expanding our efforts to explore the scope of this novel recognition mode. Finally, we note that the **G_4-PNA** oligomer should be capable of forming its own quadruplex structure in the absence of any homologous DNA. UV melting and FRET experiments will allow us to begin studying such assemblies. Of particular interest are recent reports from Davis and co-workers on the self-assembly of stacked guanine tetrads within lipid bilayers,[36] structures that the uncharged PNA oligomers might be capable of mimicking.

Acknowledgment. We are grateful to the National Institutes of Health (R01 GM-58547-02) for financial support of this research and to Dr. Brigitte Schmidt for the generous gift of Cy3-carboxylic acid. MALDI-TOF mass spectra were recorded in the Center for Molecular Analysis at Carnegie Mellon University, supported by NSF Grant CHE-9808188.

Supporting Information Available: Concentration dependent analysis of thermodynamic parameters for PNA_2-DNA_2 quadruplex formation (Figure S1) and effect of Li^+ on the thermal stability of PNA_2-DNA_2 quadruplex (Figure S2). This material is available free of charge via the Internet at http://pubs.acs.org.

JA028323D

(56) Dias, N.; Sénamaud-Beaufort, C.; le Forestier, E.; Auvin, C.; Hélène, C.; Saison-Behmoaras, T. E. *J. Mol. Biol.* **2002**, *320*, 489−501.
(57) Hultdin, M.; Grönlund, E.; Norrback, K.-F.; Erikkson-Lindström, E.; Just, T.; Roos, G. *Nucleic Acids Res.* **1998**, *26*, 3651−3656.
(58) Rufer, N.; Dragowska, W.; Thornbury, G.; Roosnek, E.; Lansdorp, P. M. *Nature Biotechnol.* **1998**, *16*, 743−747.
(59) Darnell, J. C.; Jensen, K. B.; Jin, P.; Brown, V.; Warren, S. T.; Darnell, R. B. *Cell* **2001**, *107*, 489−499.
(60) Brown, V.; Jin, P.; Ceman, S.; Darnell, J. C.; O'Donnell, W. T.; Tenenbaum, S. A.; Jin, X.; Feng, Y.; Wilkinson, K. D.; Keene, J. D.; Darnell, R. B.; Warren, S. T. *Cell* **2001**, *107*, 477−487.
(61) Zhang, Y. Q.; Bailey, A. M.; Matthies, H. J. G.; Renden, R. B.; Smith, M. A.; Speese, S. D.; Rubin, G. M.; Broadie, K. *Cell* **2001**, *107*, 591−603.
(62) Siddiqui-Jain, A.; Grand, C. L.; Bearss, D. J.; Hurley, L. H. *Proc. Natl. Acad. Sci. U.S.A.* **2002**, *99*, 11 593−11 598.